J Solid State Electrochem (2005) 9: 900–908
DOI 10.1007/s10008-005-0049-z

ORIGINAL PAPER

R. Ramanauskas · L. Gudavičiūtė · A. Kaliničenko
R. Juškėnas

Pulse plating effect on microstructure and corrosion properties of Zn–Ni alloy coatings

Received: 29 April 2005 / Revised: 1 June 2005 / Accepted: 30 June 2005 / Published online: 2 August 2005

Abstract The influence of pulse plating parameters on the surface morphology, grain size, lattice imperfection and corrosion properties of Zn–Ni alloy has been studied. The coatings were electrodeposited in an alkaline cyanide-free solution. AFM was applied for surface morphology examination, XRD measurements were carried out for phase composition and texture analysis, electron probe microanalysis was used for alloy chemical composition studies, while electrochemical techniques were applied for corrosion performance evaluation. The pulse plated Zn–Ni coatings appeared to consist of the γ-$Zn_{21}Ni_5$ phase and the composition of the alloy depended on the plating parameters. The grain size, lattice imperfection and homogeneity of grain distribution were established to be the main factors determining corrosion behaviour of the coating.

Keywords Zn and Zn alloys · Electrodeposits · Structure · Corrosion

Introduction

The corrosion resistance of conventional Zn coatings is not sufficient nowadays because of the permanent requirement of industry (especially automotive) to reduce coatings thickness and to increase corrosion resistance at the same time. Therefore, extensive attempts have been taken recently to develop highly corrosion resistant coatings on steel and as a result, the conventional Zn coatings are being replaced by Zn alloys [1–7]. It has been stated in several studies that corrosion resistance of electrodeposited Zn–Ni alloy coatings within a certain composition range (9–15 wt%) can be significantly higher (five to six times) than that for pure zinc [8–15].

Electrodeposited Zn–Ni alloys exist in the form of three dominant phases: α, γ and η. The α-phase is a solid solution of Zn in Ni with an equilibrium solubility of about 30% Zn. The η-phase is a solid solution of Ni in Zn, with a Ni solubility of less than 1%. The composition range of the pure γ-single phase was determined to be between 10 and 30% Ni. The amount of Ni in the alloy, which finds industrial application in the corrosion protection field, is around 15% and its dominant structure is the γ-phase $Zn_{21}Ni_5$ [15].

It was revealed in our previous works, [12, 16–18], that metal structure is an important parameter, which under certain conditions (corrosion product film formation) can be the main factor determining corrosion behaviour of Zn alloys. Modification of the Zn–Ni alloys' structure, therefore, may be the way to create new more resistant coatings on steel.

Pulse electrodeposition can be used as a means to produce a unique structure, i.e. coatings with properties not obtained by direct current (dc) plating. Pulse electrodeposition yields a finer grained and more homogeneous surface appearance of the deposit, because a higher instantaneous current density is possible during deposition. Pulse plating also yields uniformity in alloy composition and grain structure, smoother and denser deposits with negligible porosity.

Acidic or alkaline plating baths can be used for Zn–Ni alloy deposition. Data on pulse plated Zn–Ni alloy published till date deal with the coatings deposited from acidic solutions [15, 19–21]. Electrodeposition of this alloy in acidic bath, especially under dc condition, results in the dual phase structure formation [22], which implies an unsatisfactory corrosion resistance of the coating. Meanwhile, deposition in alkaline solutions, in contrast to acidic ones, is less efficient but gives a more uniform plating and results in the γ-single phase formation [16, 18].

The objective of the present investigation was to determine the influence of pulse electrodeposition

Presented at the 4th Baltic Conference on Electrochemistry, Greifswald, March 13–16, 2005

R. Ramanauskas (✉) · L. Gudavičiūtė · A. Kaliničenko
R. Juškėnas
Institute of Chemistry, A. Goštauto 9, 01108 Vilnius, Lithuania
E-mail: ramanr@ktl.mii.lt

parameters on the surface morphology, grain size, lattice imperfection and corrosion properties of Zn–Ni coatings deposited in alkaline bath.

Experimental

Zn–Ni (12%) coatings 10 μm thick were electrodeposited on low carbon steel (C 0.05–0.12%, Mn 0.25–0.5%) samples, which were polished mechanically to a bright mirror. An alkaline cyanide-free plating solution contained ZnO 10 gl^{-1}, NaOH 100 gl^{-1}, organic additives and a glycerine complex of Ni ions. The coatings were deposited at 25 °C under the following basic plating parameters: cathodic peak current density $i_p = 3$ A cm^{-2}, current on-time $t_{on} = 0.50$ ms, current off-time $t_{off} = 3$ ms. During the reverse current peak application the duration of anodic pulse was 0.2 ms. A detailed description of the plating bath and operating conditions is presented elsewhere [12, 16–18].

Surface morphology studies were carried out with an AFM by an Explorer (VEECO-Thermomicroscopes) scanning probe microscope at atmospheric pressure and room temperature in a contact mode. A Si_3N_4 cantilever with the force constant of 0.032 N m^{-1} was used and the resolution of the images obtained was 300×300 pixels. The grain-size dimensions of electrodeposited coatings were determined by means of SPMLab software and from profile line analysis.

X-ray diffraction measurements were performed with a D8 diffractometer equipped with a Göbel mirror (primary beam monochromator) for Cu radiation. A step-scan mode was used in the 2-θ range from 30° to 75° with a step length of 0.02° and a counting time of 5 s per step.

Chemical composition of electrodeposited Zn–Ni was determined applying electron probe microanalysis with SEM JXA-50A.

The corrosion behaviour of coatings was investigated in 0.1 M NaCl + 0.1 M $NaHCO_3$ solution (pH 6.8) using a standard three-electrode system with a Pt counter electrode, a saturated calomel reference electrode and a PI-50 potentiostat.

Results and discussion

Chemical composition

Data on the composition, structure and corrosion behaviour of Zn–Ni coatings deposited in an alkaline bath by the direct current were presented in our previous studies [16, 18]. It was established that the mentioned coatings consisted of the γ-$Zn_{21}Ni_5$ phase with the content of Ni close to ca. 12%, while their corrosion resistance under the conditions when the passivating corrosion product, film forms (atmospheric corrosion or aqueous corrosion in a Cl^- ions containing buffered solution), appeared to be significantly higher than those of pure Zn coatings [16].

The principal requirements for the pulse plated Zn–Ni alloy were the absence of pitting damages and/or dendrites on the surface of the coating and the stability of its composition. The latter condition implies a variation of Ni content in the alloy between 10 and 15%. A lower amount of Ni in the alloy is accompanied by a dual phase formation, while a higher one causes the loss of the sacrificial protection effect of the coating.

The influence of pulse and reverse plating parameters (cathodic peak current density [i_p], current on-time [t_{on}], current off-time [t_{off}] and anodic peak current density [i_a]) on the amount of Ni in the alloy are presented in Fig. 1. Electrodeposition conditions affected significantly the composition of Zn–Ni alloy. The increase in i_p and t_{off} caused an increase, while the increase in t_{on} and i_a, in contrary, led to a decrease in Ni content in the alloy. The values of i_p lower than 1 A cm^{-2} were not acceptable, because they caused reduction in Ni content below 10%, while application of t_{on} lower than 0.2 ms and i_a lower than 0.1 A cm^{-2} resulted in alloy formation with a Ni content overcoming 15%. The latter case was not acceptable in this study, either. The presented dependences (Fig. 1) validate the optimal range of pulse plating parameters, which ensured the desirable composition of Zn–Ni alloy.

Phase composition

The influence of pulse plating parameters on the phase composition of the deposited alloy can be determined from XRD data. Figure 2 shows XRD patterns of Zn–Ni coatings deposited under various i_p conditions. The variation of other pulse and reverse plating parameters (t_{on}, t_{off} and i_a) did not cause the appearance of any new characteristic features in the obtained diffractograms, therefore, they are not presented here.

All the Zn–Ni samples showed sharp peaks corresponding to the base metal (Fe) and to γ-$Zn_{21}Ni_5$ phase. No other Zn–Ni alloy phases were detected to be present in the electrodeposited coatings. This fact implies that under the applied pulse and reverse plating conditions the deposited alloy consisted of the single γ-$Zn_{21}Ni_5$ phase.

An additional diffraction line characteristic: a full width at half-maximum (FWHM) W_{FWHM} was measured and the obtained data will be presented and discussed below.

Surface morphology

Surface morphology studies of Zn–Ni coatings were based on AFM measurements. Investigations on the μm level (20×20 μm^2 scanned surface area) have shown that dc plated coatings (deposited at 0.035 A cm^{-2} current density) consisted of agglomerations of nodular

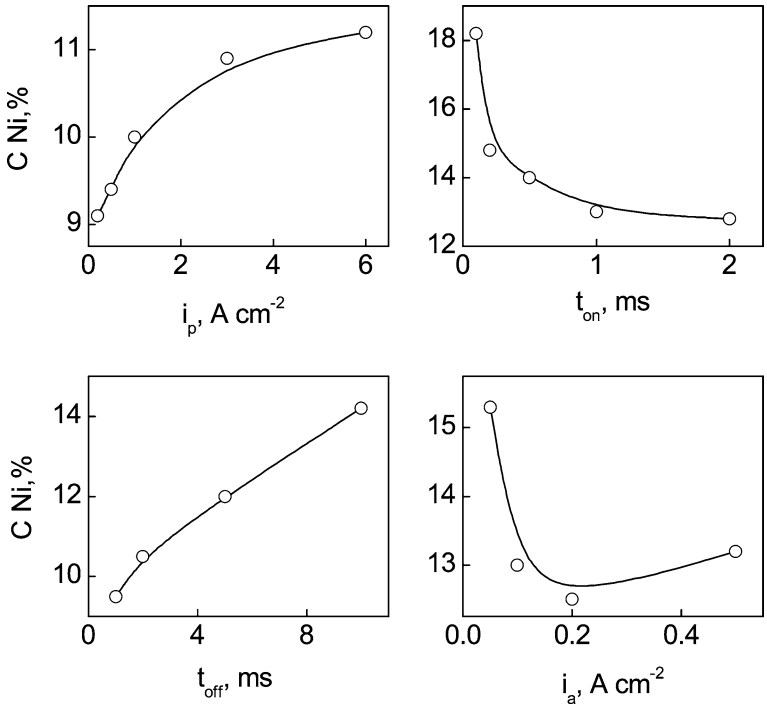

Fig. 1 Effect of pulse plating parameters on Zn–Ni alloy composition

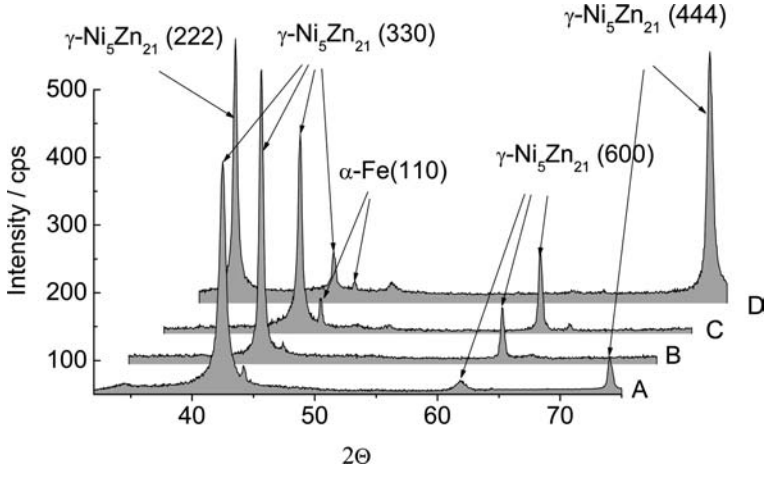

Fig. 2 XRD patterns of Zn–Ni coatings obtained by pulse plating under various cathodic current peak (i_p) densities (A cm^{-2}): *A* 0.2, *B* 1, *C* 3, *D* 6

crystallites (Fig. 3a). The dimension of such agglomerations varied between 1.1 and 3.2 μm (average 2.0 μm), meanwhile the dimensions of the individual crystallites (Δ_{cr}) ranged between 0.5 and 1.8 μm (the average value 0.92 μm).

The ultrafine-grained structure was determined from the 500×500 nm^2 scanned surface area (Fig. 4a) and the grain size (Δ_{gr}) of dc deposited coatings varied between 70 and 180 nm, with the average 90 nm value.

The influence of pulse plating parameters on the morphology of electrodeposited Zn–Ni coatings can be observed from the images presented in Figs. 3, 4, 5 and 6. The average crystallite dimensions, grain size, as well as the root-mean-square roughness (R_{rms}) values were determined from the AFM measurements and the data obtained are presented in Fig. 7 and Table 1.

The morphology of Zn–Ni alloys deposited by pulse and reverse plating appeared to depend rigorously on the plating parameters. The characteristic feature of these coatings was the lack of crystallite agglomerations, which were observed for dc plated samples. The surface of pulse plated Zn–Ni coatings appeared to consist of globular crystallites. The variation of plating caused a significant reduction in their dimensions and as a result the surface morphology underwent modification from a globular to fine-grained film.

Increase in the overpotential enhances the free energy to form new nuclei, which results in a higher nucleation rate and a smaller grain size. Therefore, an increase in i_p in the pulse plating of metals usually causes a decrease in the grain size. A similar effect was also observed for Zn–Ni pulse electrodeposits. An increase in i_p values from 0.2 to 3 A cm^{-2} caused reduction in the average Δ_{cr} values from 0.82 to 0.42 μm (Figs. 3b–d, 7) and reduction in the average Δ_{gr} from 62 to 40 nm (Figs. 4 b–d, 7). The further increase in i_p (>3 A cm^{-2}) caused decrease

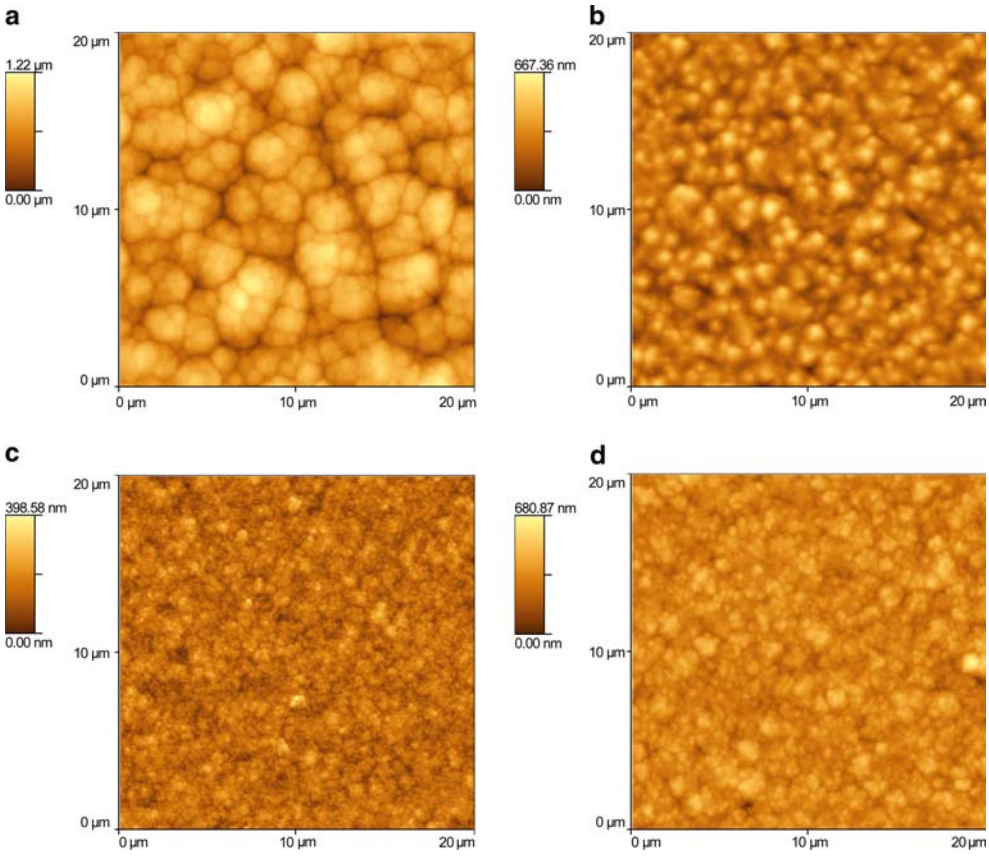

Fig. 3 Surface morphology of Zn–Ni coatings deposited under various i_p values (A cm^{-2}): **a** 0.035 (dc plated coating), **b** 0.5, **c** 3, **d** 6. The scanned area 400 µm^2

in grain size, however, with simultaneous formation of discrete large grains and crystallites (possibly germs of dendrites), which resulted in the increase in the average Δ_{cr} and Δ_{gr} values (Fig. 7). The lowest R_{rms} values of these samples varied between 60 and 40 nm and were obtained when i_p varied between 1 and 6 A cm^{-2} (Table 1).

The nucleation rate is enhanced and the grain size of deposit is usually decreased because of higher i_p, however, the effect of t_{on} and t_{off} on deposit characteristics cannot be predicted for a certain system, because the crystallization process is strongly influenced by adsorption and desorption phenomena. Therefore, each system may react differently during the electrocrystallization process yielding different surface morphology.

The variation in the t_{on} parameter enabled to obtain Zn–Ni alloys with a smoother surface, as compared with the previous (i_p) case (Figs. 5, 6a, b). The average R_{rms} values around ~20 nm were obtained when t_{on} varied between 0.2 and 1 ms. In general, the application of the t_{on} parameter higher than 0.2 ms produced Zn–Ni surface with spherical crystallites and relatively undefined grain boundaries. The influence of t_{on} on the average Δ_{cr} and Δ_{gr} appeared to be similar to that of the (i_p) case. A decrease in average of both Δ_{cr} to 0.40 µm (Fig. 5 a) and Δ_{gr} to 35 nm (Fig. 6a) was obtained at 1 and 0.5 ms t_{on}, respectively. The formation of discrete large crystallites on the alloy surface was observed when t_{on} higher than 1 ms was applied (Fig. 5b), which caused the increase in the average Δ_{cr} and Δ_{gr} values under these plating conditions (Fig. 7). The reappearance of the large crystallites at the longest t_{on} may be explained by a large duty cycle value, which is approaching dc electrodeposition.

In pulse plating there is no applied current during the t_{off} period. However, it is not dead time from the standpoint of crystallization. Whether the fine-grained deposit is obtained in practice depends upon what happens during the t_{off} period when the current is interrupted. Desorption of impurities and encouragement of renucleation with the formation of new, smaller grains can be allowed during this period. Besides, local corrosion of cells, if this period is long enough, can occur, as has been stated in [22]. The t_{off} variations influenced formation of Zn–Ni alloy coatings with the lowest values of Δ_{cr} and Δ_{gr} 0.4 µm and 40 nm, respectively (Figs. 5, 6c, d, 7). However, if in the case of i_p and t_{on} variations the average Δ_{cr} and Δ_{gr} alterations were very similar, the increase in the t_{off} values caused the decrease in Δ_{cr} values and a simultaneous slight increase in the Δ_{gr} values (Fig. 7). Some macro-structural defects as surface flaws typical of local corrosion attack were observed on the surface when t_{off} exceeded 5 ms (Fig. 5d). This fact limited the use of higher t_{off} values.

Electrolytes containing organic additives may undergo changes in the deposition mechanism when the current of the altering polarity is used. The use of anodic pulse permits not only to increase the working current density, but as a result of periodic action of

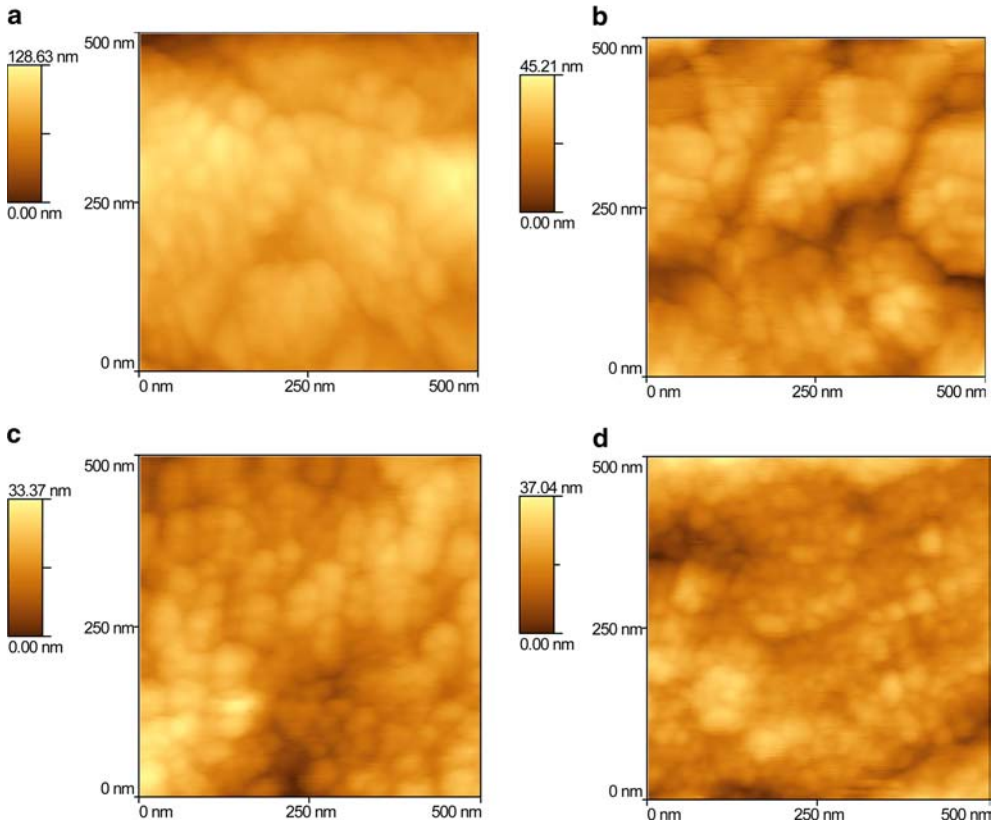

Fig. 4 Surface morphology of Zn–Ni coatings deposited under various i_p values (A cm^{-2}): **a** – 0.035 (dc plated coating), **b** – 0.5, **c** – 3, **d** – 6. The scanned area 0.25 μm^2

the anodic current on the deposited layer of metal, the deposit acquires better properties as well. For a number of processes current reversal is the means of achieving smoother, brighter and less porous deposits [22, 23].

Application of the reverse current peak produced significantly smoother, as compared to all other pulse plated Zn–Ni coatings, surfaces with R_{rms} close to 11–15 nm (Table 1, Figs. 5, 6e, f, 7). The introduction of current pulse of altering polarity in the deposition program caused the formation of spherical crystallites with relatively undefined grain boundaries, however, it permitted to refine neither significantly crystallite, nor grain size dimensions. Similarly to the t_{off} influence on coatings morphology, the increase in i_a caused the decrease in the Δ_{cr} values, while Δ_{gr} variations were not so significant. The smallest crystallites (Δ_{cr} ~0.35 μm) were obtained at $i_a \geq 0.2$ A cm^{-2}, while the lowest values of Δ_{gr} (~35 nm) were observed for coatings deposited at i_a 0.05 A cm^{-2} (Fig. 7). However, the further increase in i_a (>0.2 A cm^{-2}) caused the formation of structural defects originated most probably by the alloy ionization process (Fig. 6f).

It may be stated, therefore, that the main difference between the Zn–Ni alloys obtained with dc and those obtained with any pulse techniques is the grain size dimensions: application of pulse and reverse current in electrodeposition of Zn–Ni alloy in alkaline solution results in a significantly smoother surface with relatively indefinite grain boundaries and a reduction in the grain size from ca. 90 nm for dc plated up to 35–40 nm for pulse plated samples.

Relationship between corrosion behaviour and metal structure

Corrosion behaviour of pulse plated Zn–Ni coatings was investigated in a naturally aerated NaCl + $NaHCO_3$ solution at pH 6.8 by means of anodic polarization measurements. It is known, however, that the corrosion rates measured electrochemically are in error with atmospheric data, mainly because of the presence of corrosion products on the surface. Zn alloy corrosion in unbuffered Cl^- solution occurs with the formation of oxide film having a porous structure [24]. However, in HCO_3^- containing media the oxide film is supposed to be more compact, adherent and less soluble, thus exhibiting a passivating character [25]. Aqueous corrosion data for Zn alloys in HCO_3^- containing media correlate well with atmospheric corrosion data [16]. The corrosion currents were determined from Tafel plot extrapolation and the data obtained are presented in Fig. 8. The same figure contains data on W_{FWHM} of the diffraction line (110) of Zn–Ni alloys electrodeposited under various conditions.

The relationship of surface morphology and corrosion behaviour (i_{corr}) of Zn–Ni coatings is not unambiguous. Generally, the lower values of Δ_{cr} and Δ_{gr} yield lower i_{corr} values, as it can be observed from i_p and t_{on} variations. However, several exceptions can be observed

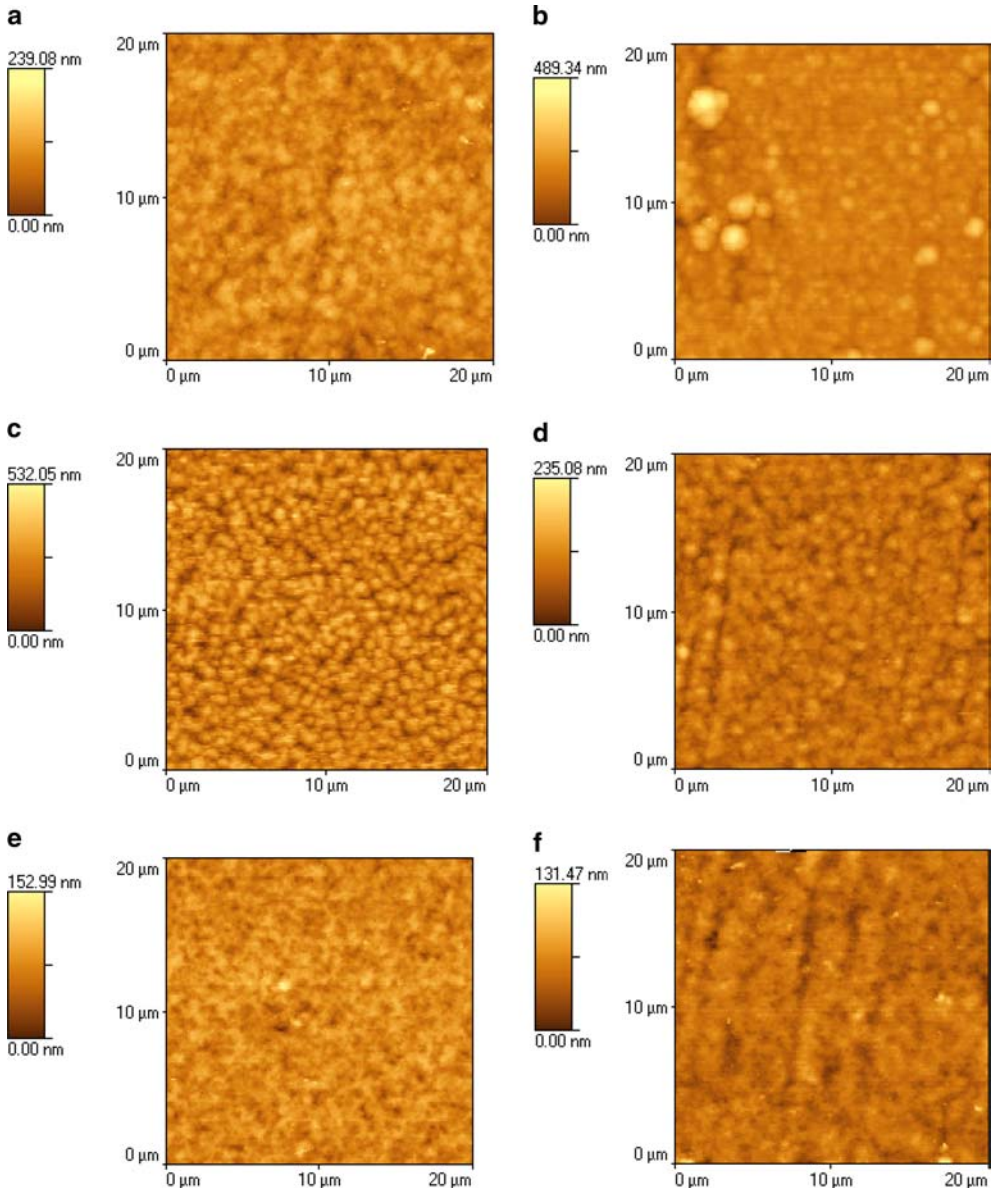

Fig. 5 Surface morphology of Zn–Ni coatings deposited under various plating conditions t_{on} (ms): **a** 0.5, **b** 2; t_{off} (ms): **c** 2, **d** 10; i_a (A cm^{-2}): **e** 0.1, **f** 0.5. The scanned area 400 µm^2

as well. For example, the increase in t_{off} from 1 to 10 ms was accompanied by the reduction in Δ_{cr} from 0.85 to 0.40 µm, meanwhile the increase in Δ_{gr} from 40 to 58 nm and corresponding increase in i_{corr} from 4×10^{-6} to 1.7×10^{-5} A cm^{-2} were observed under the same conditions. This fact implies the dominant influence of the grain size on the corrosion behaviour of Zn–Ni.

The lowest values of Δ_{gr} for electrodeposited Zn–Ni alloy under all applied plating conditions varied around 35–40 nm, while the corresponding i_{corr} values ranged between 1.5 and 4.0×10^{-6} A cm^{-2}, being the minimal ones for samples deposited with a pulse and reverse current. It seems that the grain size of the alloy alone is not responsible for the corrosion properties of the coating.

The corrosion process is essentially a surface phenomenon, thus, it might be strongly related to crystalline perfection, e.g. highly stepped metal surfaces, since the presence of dislocations makes the steps indestructible. It is reasonable hence, to argue that the lattice distortions must be important in the corrosion process. X-ray diffraction line broadening is recognized to be caused by crystallite size and lattice strains [26, 27]. It was revealed in our previous studies on the relationship of Zn electrodeposit structure and their corrosion behaviour that the observed line broadening is affected mostly by lattice imperfections [16, 18]. Therefore, it was reasonable to analyse W_{FWHM}, which indicates diffraction line breadth, and i_{corr} correlation.

As evident from the data presented in Fig. 8 Zn–Ni coatings, which exhibited lower i_{corr} values, at the same time possessed higher values of W_{FWHM} and vice versa. For example, the increase in i_p from 0.2 to 3 A cm^{-2} resulted in the formation of Zn–Ni alloy with W_{FWHM}

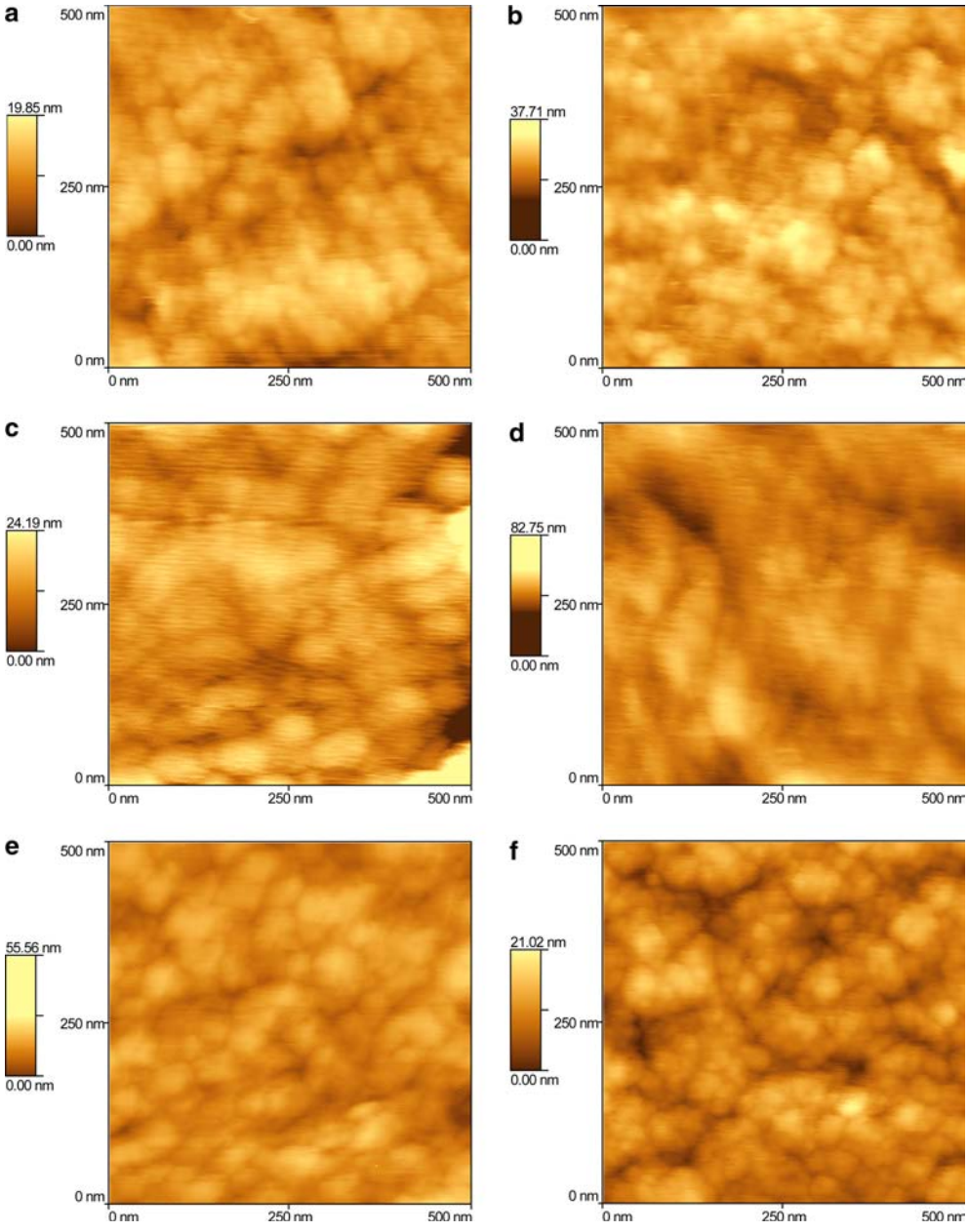

Fig. 6 Surface morphology of Zn–Ni coatings deposited under various plating conditions t_{on} (ms): **a** 0.5, **b** 2; t_{off} (ms): **c** 2, **d** 10; i_a (A cm^{-2}): **e** 0.1, **f** 0.5. The scanned area 0.25 μm^2

increasing from 0.665° to 0.690° and i_{corr} decreasing from 7×10^{-6} to 3×10^{-6} A cm^{-2}, respectively. Meanwhile, the increase in t_{off} from 1 to 10 ms resulted in decrease of W_{FWHM} values from 0.77° to 0.38° and simultaneous augment of i_{corr} from 4×10^{-6} to 1.7×10^{-5} A cm^{-2}, respectively. The fact that coatings with higher values of W_{FWHM} exhibit lower corrosion rates implies that coatings with a higher number of lattice imperfections possess higher corrosion resistance. A similar assumption was made in our previous works [16, 18, 23] with the following explanation. A decrease in crystalline perfection affects the surface reactivity and usually increases it. A higher surface activity of certain Zn–Ni alloys, and hence the metal structure, might be the precursor for oxide film formation with a high content of Zn hydroxide and poor crystallinity. The amorphous structure and lower electron conductivity of a hydrated Zn oxide compared to those of Zn oxide made such alloys more stable in corrosion environments where passive films formed on the metal surface.

However, not all pulse plating parameters applied produced coatings, which held the mentioned W_{FWHM} and i_{corr} relationship. For example, a slight increase in W_{FWHM} from 0.690° to 0.695° was observed for Zn–Ni samples deposited under i_p 3 and 6 A cm^{-2}, which was accompanied by a drastic increase in i_{corr} from 3×10^{-6} to 2.5×10^{-5} A cm^{-2}, respectively. The manifesting discrepancies are most probably related to lower homogeneity of grain distribution, which were originated from the appearance of discrete large grains when i_p exceeded 3 A cm^{-2} or t_{on} exceeded 1 ms. For example, if to compare morphology of coatings deposited under i_p 1

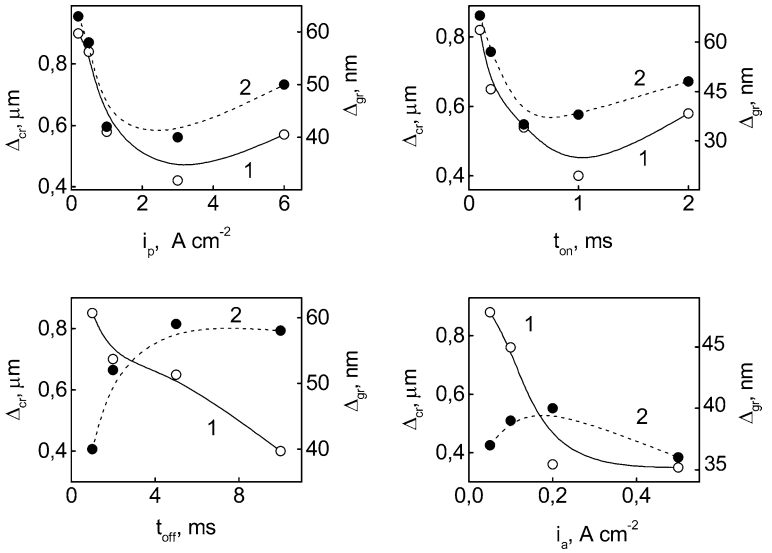

Fig. 7 Effect of pulse plating parameters on the crystallite radius (Δ_{cr}, μm) (*1*) and grain size (Δ_{gr}, nm) (*2*) of pulse plated Zn–Ni coatings

Table 1 Root-mean-square roughness (R_{rms}) of pulse and reverse plated Zn–Ni coatings

Electrodeposition	Parameter	R_{rms} (nm)
i_p (A cm^{-2})	0.2	144
	0.5	82
	1	52
	3	40
	6	61
t_{off} (ms)	1	48
	2	58
	5	45
	10	30
t_{on} (ms)	0.1	84
	0.2	21
	0.5	23
	1	20
	2	37
i_a (A cm^{-2})	0.05	13
	0.1	11.5
	0.2	13.5
	0.5	15

and 6 A cm^{-2} it can be stated that the average grain size of both deposits did not differ greatly and was close to 45 nm, while W_{FWHM} values were even higher for sample deposited with higher i_p, however, the homogeneity of grain distribution for the latter samples was lower (Fig. 9) and corresponding corrosion currents were higher.

The appearance on Zn–Ni surface areas of local corrosion attack during reverse current cycle or time-off period may also be the reason for discrepancy in the observed relationship between W_{FWHM} and i_{corr}. Higher corrosion rates and W_{FWHM} values of samples deposited at i_a 0.5 A cm^{-2} in comparison to that one deposited at i_a 0.1 A cm^{-2} are good examples of such occurrences.

The complexity of real system makes it difficult to evaluate individually the influence of structural parameters on metal corrosion behaviour, however, the data on pulse plated Zn–Ni alloys obtained indicate that coatings possessing lower grain size, higher uniformity

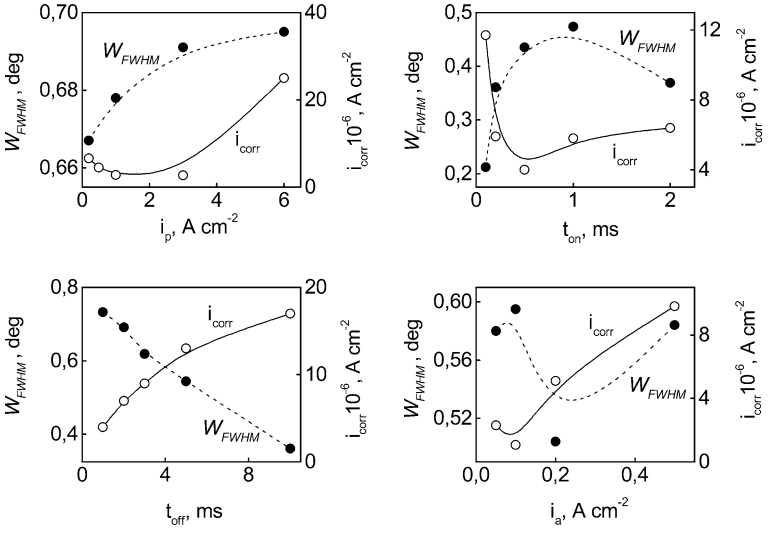

Fig. 8 Effect of pulse plating parameters on the corrosion current (i_{corr}) of Zn–Ni alloy coatings in NaCl + $NaHCO_3$ solution and the values of a full width at half-maximum (FWHM) W_{FWHM} of the diffraction line (110)

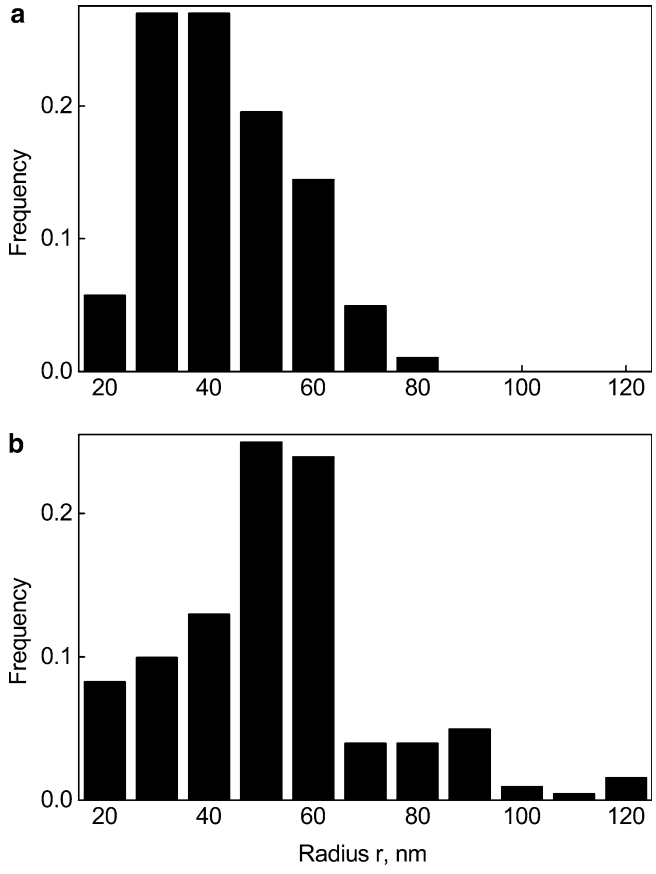

Fig. 9 Grain size distribution of Zn–Ni alloy electrodeposited with i_p values (A cm^{-2}): **a** 1, **b** 6

of grain distribution and higher number of lattice imperfections exhibit a higher corrosion resistance.

Conclusions

The composition of pulse plated Zn–Ni alloy coatings depended on the plating parameters: an increase in cathodic current peak density and time-off period caused an increase, while an increase in anodic (reverse) current peak density and time on period a decrease in Ni content in the alloy. All pulse plated Zn–Ni coatings, in spite of the differences in their composition, consisted of a single γ-Zn–Ni phase.

Pulse and reverse plating of Zn–Ni alloy in alkaline solutions resulted in the formation of a significantly smoother surface with relatively indefinite grain boundaries and reduction in the grain size from ~90 nm for dc plated up to 30–40 nm for pulse plated samples.

Zn–Ni alloys, which possessed lower grain size, higher uniformity of grain distribution and higher number of lattice imperfections exhibited a higher corrosion resistance. Appearance of macro-structural defects, such as areas of local corrosion attack or large grains, was the reason for higher corrosion activity of electrodeposited coatings.

References

1. Muller C, Sarret M, Andreu T (2003) Electrochim Acta 48:2397
2. Bahrololoom ME, Gabe DR, Wilcox GD (2003) J Electrochem Soc 150:C144
3. Tsuru Y, Egawa H (1997) Denki Kagaku 65:143
4. Zhang Z, Leng WH, Shao HB, Zhang JQ, Wang JM, Cao CN (2001) J Electroanal Chem 516:127
5. Bajat JB, Mislovic-Stankovic VB, Maksimovic MD, Drazic DM (2002) Electrochim Acta 47:4101
6. Younan MM (2000) J Appl Electrochem 30:55
7. Ashassi-Sorkhabi H, Hagrah A, Parvini-Ahmadi N, Manzoori J (2001) Surf Coat Technol 140:278
8. Baldwin KR, Robinson MJ, Smith CJE (1993) Corros Sci 35:1267
9. Fedrizzi L, Fratesi R, Lunazzi G, Roventi G (1992) Surf Coat Technol 53:171
10. Wilcax GD, Gabe DR (1993) Corros Sci 35:1251
11. Kautek W, Sahre M, Paatsch W (1994) Electrochim Acta 39:1151
12. Pech-Canul MA, Ramanauskas R, Maldonado L (1997) Ibid 42:255
13. Bajat JB, Maksimovic MD, Miskovic-Stankovic VB, Zec S (2001) J Appl Electrochem 31:355
14. Hu Ch, Tsay Ch, Bai A (2003) Electrochim Acta 48:907
15. Alfantazi AM, Page J, Erb U (1996) J Appl Electrochem 26:1225
16. Ramanauskas R Appl Surf Sci 153:53
17. Ramanauskas R, Gudaviciute L, Diaz-Ballote L, Bartolo-Perez P, Quintana P (2001) Surf Coat Technol 140:109
18. Ramanauskas R, Juskenas R, Kalinicenko A, Garfias-Mesias LF (2004) J Solid State Electrochem 8:416
19. Alfantazi M, Erb U (1996) Corrosion 52:880
20. Tsuru Y, Tanaka M (1996) Denki Kagaku 64:112
21. Kondo K, Yokoyama M, Shinohara K (1995) J Electrochem Soc 142:2256
22. Mandich NV (2000) Metal Finish 98:375
23. Gudavičiūtė L, Kaliničenko A, Juškėnas R, Ramanauskas R (2004) Chemija 15:22
24. Graedel TE (1989) J Electrochem Soc 136:193C
25. Guo R, Weinberg F, Tromans D (1995) Corrosion 51:356
26. Balzar DJ (1992) J Appl Cryst 25:559
27. Giridhar J, Ooij WJ (1992) Surf Coat Technol 52:17